ISSN 1070-4272, Russian Journal of Applied Chemistry, 2023, Vol. 96, No. 2. pp. 245–257. © Pleiades Publishing, Ltd., 2023.

PROCESSES AND EQUIPMENT OF CHEMICAL INDUSTRY

The Math Correlation of Material Chemistry and Physical Factors on Phase Inversion in the Separation of Aqueous and Organic Phases in an Agitated Vessel

Masoomeh Hajikarimian[a],* and Milad Sheydaei[b]

[a] *School of Chemical Engineering, College of Engineering, University of Tehran, Iran*
[b] *Faculty of Polymer Engineering, Sahand University of Technology, Tabriz, Iran*
**e-mail: hajikarimian@ut.ac.ir*

Received May 10, 2023; revised July 20, 2023; accepted July 20, 2023

Abstract—Phase inversion phenomenon is important in design of liquid–liquid extraction systems. In this study, the effects of the impeller speed, the hold up of dispersed phase, and surface active agent concentration on phase inversion phenomenon for toluene–water and butanol–water with sodium dodecyl sulfate (SDS) as surface active agent, were investigated. Based on the experiments in this work, some models are developed for the impeller speeds when the phase inversion phenomenon has been occurred (N_{PI}). Comparison between models for toluene–water and butanol–water systems with paddle and propeller blades, with and without SDS has been done. The dispersed to continuous phase ratios (volumetric ratio of toluene to water) were divided into three regions $V_T/V_W < 0.5$, $0.5 < V_T/V_W < 1$, and $V_T/V_W > 1$. It was found that by increasing the impeller speed and also the ratio of dispersed to continuous phase the separation time and the occurrence probability of the phase inversion phenomenon were increased. Moreover, by increasing the volumetric ratio of the dispersed to the continuous phase the separation time was raised and at a specific impeller speed the separation time did not depend on the impeller speed. By increasing the concentration of SDS up to 40 mg, the phase inversion phenomenon occurred at higher impeller speeds. In the same surface active agent concentration, the impeller speed for the phase inversion occurrence by paddle blade was higher than propeller blade.

Keywords: agitated tank, phase inversion, impeller speed, surface active agent, mixer–settler

DOI: 10.1134/S1070427223020168

INTRODUCTION

Agitated extraction tanks (batch mixer settlers) are interesting because of their high capacity, flexibility, and efficiency. They widely utilized in various processes such as chemical, biochemical, drug, food and nuclear industries [1–3]. In a liquid–liquid system which is comprised of two immiscible liquids (for instance an aqueous solution phase with an organic solution phase) according to the state of the system, two types of dispersion can be observed; one of them is the dispersion of oil-in-water (O/W) formed by dispersal of oil drops in water, and the next dispersion is water-in-oil (W/O) which is shaped by dispersal of water drops in oil [4–6]. Phase inversion is defined as the phenomenon whereby the phases of a liquid–liquid dispersion interchange so that the dispersed phase during mixing inverts to become the continuous phase and vice versa, under conditions that are determined by the system properties and operational parameters such as impeller speed, phase volume ratio, energy input, container geometry, presence of mineral compounds, the interfacial tension and the density difference between two liquids, the initial conditions of flow systems as well as temperature [7]. As mentioned above a lot of parameters can influence the inversion phenomenon and several physical mechanisms have been postulated to explain phase inversion. In one of the most well-known mechanisms phase inversion was regarded as instability between breakup and coalescence of dispersed drops. Therefore, phase inver-

sion can be assumed to be an unstable state where the system cannot maintain the dynamic balance between breakup and coalescence, and the ambivalent range corresponds to the difference of coalescence and breakup potential in the aqueous and organic continuous dispersions [8–10]. The point at which phase inversion occurs corresponds to the holdup of the dispersed phase for a system at which the transition occurs after an infinitesimal change is made to the properties of the system [11, 12]. Consequently, phase inversion is an important phenomenon to be considered in liquid–liquid systems, since it represents the instability of a system and may affect separation of two immiscible phases. On the other hand, determination of the inversion point is necessary to maintaining a proper dispersion, because in some operations, especially in mixer–settlers, spontaneous inversion can be highly undesirable. Due to the complex behavior of liquid dispersions and mass transfer processes related to it, the experimental data are necessary for mixer–settlers design. Two types of phase inversion experiments are reported in the literature: continuous experiments and direct experiments. During a continuous experiment the dispersed phase is gradually added to the continuous phase and so the volume fraction of the dispersed phase increases with time. During a direct experiment the two liquids are mixed from the start at certain values of the phase volume fraction for the two phases, which remain constant with time. The phase inversion phenomenon was first investigated by Rodger et al. [13]. After that Selker and Sleicher showed the existence of a hysteresis effect between inversion from an organic and from an aqueous continuous solution which was refers to ambivalent region [14]. Kato et al. experimentally illustrated the different dispersion types in agitated liquid–liquid systems [15]. Efthimiadu et al. worked on different aspects of ambivalent region [16]. Miller et al. studied about the effect of hydrophilic emulsifier on phase inversion [17]. They used emulsifier combination rapeseed sorbitol ester (hydrophobic) and lauroyl glutamate (hydrophilic). Yeo et al. worked on prediction of phase inversion and the influence of the Marangoni on phase inversion behavior by integrating a microscopic study of the drop coalescence process, in which thin film drainage in the presence of insoluble surfactant occurs, into a macroscopic phase inversion model which has been developed previously using a Monte Carlo technique [18, 19]. Brauner and Ullmann combined the criterion of minimum free energy of the system with a model for drop size in dense dispersions to predict the critical conditions for phase inversion [20]. Sajjadi et al. investigated phase inversion behavior of a model oil-water emulsion, *p*-xylene–water, with Span 20/Tween 20 as a surfactant set [21]. Deshpande and Kumar recommended that the inversion holdup for sufficiently turbulence is independent of all the operational parameters of a stirred tank [22]. Bouchama et al. worked on catastrophic phase inversion and the experiments were carried out in a stirred vessel where phase inversion was detected by a jump in emulsion conductivity [23]. Liu et al. carried out experimental investigation on the phase inversion using laser-induced fluorescence (LIF) [24]. By using two-region model, Hu et al. predicted the phase inversion in agitated vessels [25]. Ioannou et al. studied phase inversion and its effect on pressure gradient during the dispersed flow of two immiscible liquids for two pipe materials (steel and acrylic) and two pipe sizes [26]. In another study, in order to predict the phase inversion, the population balance equations with the equal surface energy in liquid–liquid dispersed pipeline flows was utilized [27]. Piela et al. performed an experimental study about phase inversion in an oil-water flow through a horizontal pipe loop [28]. Amouei et al. performed some experimental investigations on the phase inversion include of components such as toluene, *n*-heptane, NaCl, and $MgSO_4$ and they found that adding salt to an O/W dispersion enhanced the phase inversion which was more obvious for salt with a higher charge [29]. Hedayat et al. illustrated a theoretical model based on simple assumptions to predict the phase inversion point, ambivalence region and the hysteresis effect of inversion [30]. Piela et al. studied the effect of addition of a surfactant or of a salt on the critical dispersed phase volume fraction [31]. Mandal et al. described phase inversion during kerosene–water flow through a 0.012 m diameter horizontal pipe [32]. Hapanowicz studied the phase inversion phenomenon which occurs when an unstable, two phase liquid–liquid system flows through a horizontal pipe [33]. Xu et al. attempted to investigate about phase inversion and frictional pressure gradients during simultaneous vertical flow of oil and water two-phase through upward and downward pipes [34]. Preziosi et al. performed an experimental investigation on phase inversion emulsification to produce stable samples. The authors used direct observation via optical and confocal microscopy to characterize the emulsion morphology in

detail [35]. Assadabadi et al. investigated the effects of silica nano-particles on phase inversion of liquid–liquid dispersions in a stirred vessel for toluene dispersed in water and vice versa [36]. The results indicated that increase in silica nano-particle concentrations up to 0.07 wt % led to increase in agitation speed of phase inversion 43–53.5% and 38.5–45% in the case of O/W and W/O dispersions, respectively. Wang et al. used population balance equations to model and predict the drop diameter distribution of dispersed Exxsol D80 oil-in-water in a lab scale stirred tank [37]. Perazzo et al. presented a valuable review paper about various aspects of phase inversion phenomena and its applications and weaknesses and Holda and Vankelecom wrote another review paper about phase inversion process recognition and guidance for solvent resistant nano filtration membrane synthesis [38, 39]. Soin et al. used phase inversion method to fabricate self-polarized polyfluoride vinylidene films whereby quenching temperature technique from 100 to –20°C, respectively, to control polymorphism of films [40]. Li et al. used phase inversion wherein high temperature sintering to preparing a low-cost alumina-mullite composite hollow fiber ceramic membrane, and Munirasu et al. by using this technique with alcohols formed highly porous and super hydrophobic polyvinylidene fluoride membrane, for desalination or membrane distillation [41, 42]. Based on the fact that some of essential oils, such as those extracted from cinnamon, are effective natural antimicrobial substances, but because of their low water-solubility are of limited usage, and on the theory that manufacture of nanoemulsions can be accomplished by improving in oil phase compound and level of the surfactant, and its stability can be increased by cooling-dilution process at the phase inversion temperature, Chuesiang et al. used phase inversion point to prepare and stabilize the cinnamon nanoemulsions and investigated the effect of the oil phase compound and the surface active agent level on the formation and stability of the nanoemulsions [43]. Honse et al. observed phase inversion in a model emulsion [water/(heptane–toluene)] and crude oil by spectroscopy and electrical methods and applied near-infrared spectroscopy and principal component analysis to detect the phase inversion of emulsions in crude oil and found that this technique is very successful in detecting phase inversion especially in complex systems such as crude oil [44]. Pierlot et al. experimentally worked on catastrophic phase inversion of the water/alkyd resin system containing a hydrophilic nonionic surfactant and detected that by monitoring, torque measurement and the electrical conductivity, until an equal weight fraction of water and resin [45]. Binks and Shi worked on the preparation of a polymer/polymer aqueous two-phase system (ATPS), polyethylene glycol/Na_2SO_4, by solid particles and monitored phase inversion phenomenon and evolution of emulsion stability along the mapped tie lines and found the stability to coalescence caused to decrease approaching conditions of phase inversion [46]. In spite of the many studies on this field, basic understanding of the mechanism leading to phase inversion has not yet been completely discovered and there are some theories for phase inversion mechanism [38, 39]. Due to the complex behavior of liquid dispersions and mass transfer processes, the experimental data are essential for mixer–settlers design purposes. In addition, the stability of a dispersion phase is the most important parameter in a liquid–liquid extraction process which must be investigated [11, 46]. In this paper, by using the direct visualization method and electrical conductivity measurements at a specific volumetric ratio of dispersed to continuous phase in liquid–liquid dispersion, some behavior of phase inversion phenomenon and the effect of impeller speed and surface active agent concentration on the phase inversion were studied in a vessel using continuous experiments (for phase inversion and separation time investigations) and direct experiments (for surface active agent investigations). N_{PI} means the impeller speeds at which phase inversion phenomenon has been occurred, was determined. Also, several experiments are performed to investigate the effects of impeller speed on the separation time. In this study phase inversion, separation time, and effect of surface active agent on the toluene–water system is investigated. In order to study the foregoing parameters, experimental curves of two types of impellers, i.e., paddle and propeller blades are compared in the toluene–water–SDS system. In addition, due to the difficulties in understanding the mechanism which is responsible for phase inversion, the ability to predict the inversion point is severely limited. After that according to experimental study results, using the nonlinear least squares (NLS) method some simple models are illustrated for the impeller speeds in which phase inversion phenomenon has been occurred. In order to perform the modeling, toluene–water and butanol–wa-

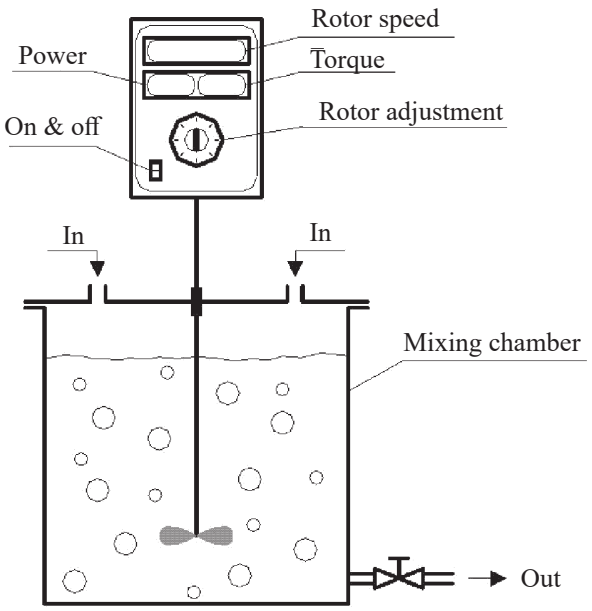

Fig. 1. Batch mixer–settler.

ter systems with paddle and propeller blades, with and without surface active agent (SDS) have been considered.

EXPERIMENTAL

Characteristics of setup and chemical system. The unit used in this study is a batch mixer–settler system, equipped by a variable speed driver and a RZR2102 controller (Heidolph Company of Germany). The container of the mixer–settler was a vertical cylinder with 0.5 L volume. The impeller speed was digital, so it could be easily controlled. The schematic of tank and mixer are illustrated in Fig. 1. The characteristics of utilized tank and blades are summarized in Table 1.

Table 1. Characteristics of mixer–settler utilized in this study.

Characteristics	Vessel	First blade	Second blade
Width, m	–	0.015	0.012
High, m	0.268	–	–
Diagonal, m	–	0.07	0.05
Type	Cylindrical	Propeller	Paddle
Substance	Glass	Plastic	Steel
Thickness, m	0.005	–	–
Outer diagonal, m	0.177	–	–

Occurrence of inversion phenomenon. At first in order to prevent the further solubility and mass transfer during the experiments, toluene and butanol were solved in water. Then water was separated from toluene and butanol, and then 1 L water saturated with toluene was added to the tank. In each certain concentration of SDS, various volumes of toluene saturated with water (light phase or dispersed phase) were added to water and this procedure was repeated for butanol–water system exactly. Each ratio of toluene to water and butanol to water were mixed by both propeller and paddle blades. In order to disperse one phase in another a minimum impeller speed is required. This speed depends on mechanical properties of vessel, impeller geometry, and type of fluid, and etc which was mentioned in various references [47]. Various experiments were performed using different volumes of toluene and butanol, impeller speeds, and surface active agent concentrations. In each certain concentration of SDS and for each type of paddle, the first and the last experiments were carried out by 0.1 and 0.2 L of both toluene and butanol, respectively. All of the experiments were done with constant volume of water 1 L and the impeller speed was changed from 80 to 600 rpm. Added SDS concentrations to the toluene–water system varied from 0 to 0.05 g and to the butanol–water system varied from 0 to 0.001 g. The surface active agent measured using a balance by accuracy about ±0.00001 and added to the agitated vessel slowly. All the experiments were done at 25°C temperature and 1 atm pressure. As it mentioned before, in each test (i.e. in each specific concentration of surface active agent), the impeller speed was changed and after reaching to steady state condition the occurrence of phase inversion phenomenon was investigated using the electrical conductivity measurement. Consequently, in each certain holdup and concentration of surface active agent for each blade and both chemical systems the impeller speed is changed and after reaching to the steady state condition the electrical conductivity of the system is measured by conductivity meter. As the electrical conductivity of water is more than that of toluene and butanol, while the conductivity meter show the high conductivity, the water phase in continuous phase and the other phase is dispersion. Therefore, when a sudden decrease in conductivity is showed the inversion phenomenon has occurred and the impeller speed for this conductivity reduction is recorded. In phase inversion phenomena there is a hysteresis

effect between inversion from an organic and from an aqueous continuous solution, which manifests itself by the formation of a so-called ambivalent region, i.e. the range of organic (or dispersed) phase volume fraction wherein either the organic or the aqueous phase can be continuous [25]. It should be noted that, in order to reach the steady state condition in each specific impeller speed, a time gap was considered for the system, and then the mixer was turned off. Then the separation time of two phases was measured (separation time of two phases is defined as a needed time that reveals interfacial between water and toluene after pausing the mixer). The properties of implemented experiments by propeller and paddle blades were summarized in Tables 2 and 3, respectively. In these tables N_{PI} is the impeller speeds at which phase inversion phenomenon has been occurred.

Table 2. Characteristics of performed experiments by toluene–water–SDS system and propeller blade

SDS, g	N_{PI}, rpm	Experiment stage
0	160	1
0.005	180	2
0.01	180	3
0.015	200	4
0.02	220	5
0.03	240	6
0.04	300	7

Table 3. Characteristics of performed experiments by toluene–water–SDS system and paddle blade

SDS, g	N_{PI}, rpm	Experiment stage
0	220	1
0.005	300	2
0.01	320	3
0.015	340	4
0.02	360	5
0.03	420	6
0.04	500	7

Model development. According to the experiments in this work, some models are developed for the impeller speeds at which phase inversion phenomenon has been occurred. The comparison between models for toluene–water and butanol–water systems with paddle and propeller blades, with and without surface active agent (SDS) has been done. The modeling was performed by EViews software. EViews is an interactive program, which provides a tool to do the best detailed data analyses, particularly in developing and evaluating models, in doing residual analysis and in testing various hypotheses, either univariate or multivariate hypotheses, estimation, and forecasting. Specially, EViews, can be use for manipulating time series data since it was originally the time series processor (TSP) software for large mainframe computers [48]. There are many alternative time series models which could be defined or developed based on only a set of three or five variables. One of the most popular models is models which was used in the present work [49]. In this investigation the functional relationship of N_{PI} and independent variables is based on regression analysis of data of time series and scientific theories. In some cases maybe one or some selected variables do not have considerable effect on the model and on the other hand, their values are zero or near to zero. The probability of this issue can be confirmed by EViews utilization and is appeared in the results by prob (*t*-Statistic) and prob (*F*-Statistic) items. prob (*t*-Statistic) shows the probability that the variable value is zero. If the value of this parameter for a variable is less than 0.05 this fact denotes that the coefficient can not be eliminated. There is a probability that no one of the variables have any significance effect on the model, this issue can be realized by the prob (*F*-Statistic). If the value of this parameter is less than 0.005 it means that the model covers all the independent variables well. One of the valuable criteria for checking the reliability and results comparison of a regression model with independent variables is *R*-Square (R^2). *R*-Square is the proportion of variation in the dependent variable (*Y*) that can be explained by the predictors (*X* variables) in the regression model. As predictors (*X* variables) are added to the model, each predictor will explain some of the variance in the dependent variable (*Y*) simply due to chance. One could continue to add predictors to the model which would continue to improve the ability of the predictors to explain the dependent variable, although some of this increase in *R*-Square would be simply due to chance variation then by increasing the number of independent variables the amount of R^2 raise too. The adjusted *R*-squared value is never larger than R^2, it can decrease as independent variables are added and, for poorly fitting models, it may be negative [50]. The adjusted *R*-square attempts to yield a more honest

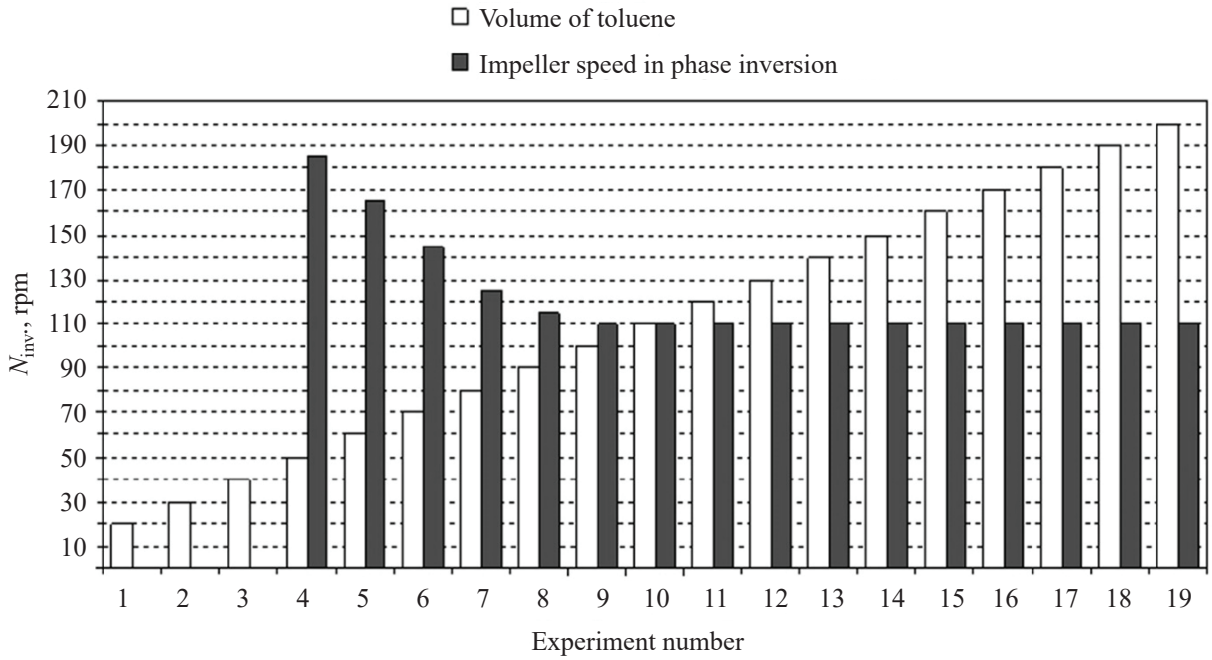

Fig. 2. Effect of impeller speed and light phase volume on inversion phenomenon.

value to estimate *R*-square. The small difference between *R*-square and adjusted *R*-square show the reliable results for the model. The Durbin–Watson test is a statistical test used to detect the presence of autocorrelation (a relationship between values separated from each other by a given time lag) in the residuals (prediction errors) from a regression analysis. If the Durbin–Watson test amount is substantially less than 2, there is evidence of positive serial correlation. As a rough rule of thumb, if Durbin–Watson is less than 1.0, there may be cause for alarm. Small values of Durbin–Watson indicate successive error terms are, on average, close in value to one another, or positively correlated. In order to have more criteria for the reliability of the model results the average absolute relative deviation (AARD%) can be used by the following equation:

$$\text{AARD} = \frac{N_{\text{PI(exp)}} - N_{\text{PI(calc)}}}{N_{\text{PI(exp)}}} \times 100, \quad (1)$$

where, $N_{\text{PI(exp)}}$ is actual impeller speed of phase inversion and $N_{\text{PI(calc)}}$ is model impeller speed of phase inversion. For the systems under experimental study the following general equation has been considered:

$$f\left(N_{\text{PI}},\ \Phi,\ \sigma, C_{\text{SDS}}\right) = 0 \Rightarrow N_{\text{PI}} = k\left(\Phi\right)^{a}\left(\sigma\right)^{b}\left(C_{\text{SDS}}\right)^{c}, \quad (2)$$

where Φ is dispersion phase holdup, C_{SDS} is the concentration of surface active agent, and σ is interfacial tension between phases. The constants *a*, *b*, *c*, and *k* are computable by various methods in optimum conditions. The model has been considered for toluene–water and butanol–water system with and without SDS.

RESULTS AND DISCUSSION

Experiments. Simultaneous effects of impeller speed and volume of light phase on inversion phenomenon is illustrated in Fig. 2, where the bar chart is the result of experiments using 19 different volumes of dispersion phase and each experiment was carried out for 15 various propeller speeds. Therefore, this chart corresponds to 19 × 15 tests for different volumes and impeller speeds. According to Fig. 2, since for toluene to water volumetric ratios less than 0.5 ($V_T/V_W < 0.5$) the governing factor of inversion phenomenon was not the impeller speed. It must be mentioned that the range closely depends on the operational and hydrodynamic conditions. For toluene to water volumetric ratios, greater than 0.5 and less than 1.0 ($0.5 < V_T/V_W < 1$), the probability of inversion phenomenon occurrence increased. For toluene to water volumetric ratios, above 1.0 ($V_T/V_W > 1$), in all cases, the inversion phenomenon took place at agitations more than 110 rpm (it must be noted that in agitations less than 100 rpm, phases do not mix together). In all states ($V_T/V_W < 1$ and $V_T/V_W > 1$), for a specific volume of toluene to water, by increasing the impeller speed the possibility of inversion phenomenon was amplified respectively, with

Table 4. Characteristics of experiments for water/toluene system.

N_{PI}, rpm	V_T/V_W	V_W, L	V_T, L	Exp.
–	0.2	0.1	0.02	1
–	0.3	0.1	0.03	2
–	0.4	0.1	0.04	3
185	0.5	0.1	0.05	4
165	0.6	0.1	0.06	5
145	0.7	0.1	0.07	6
125	0.8	0.1	0.08	7
115	0.9	0.1	0.09	8
110	1.0	0.1	0.1	9
110	1.1	0.1	0.11	10
110	1.2	0.1	0.12	11
110	1.3	0.1	0.13	12
110	1.4	0.1	0.14	13
110	1.5	0.1	0.15	14
110	1.6	0.1	0.16	15
110	1.7	0.1	0.17	16
110	1.8	0.1	0.18	17
110	1.9	0.1	0.19	18
110	2.0	0.1	0.2	19

the exception of volumetric ratios less than 0.5 in which no inversion phenomenon observed at different impeller speeds. Characteristics of experiments have been shown in Table 4. In this table N_{PI} represents the impeller speed in which the phase inversion phenomenon occurred.

The effects of impeller speed on separation time in various volumetric ratios of toluene to water are demonstrated in Fig. 3. As can be seen, since in each specific volumetric ratio of toluene to water, by increasing the impeller speed the size of drops reduced and their numbers increased significantly, consequently the separation time was raised exponentially. In other words, the time of drops coalescence was increased and ultimately, separation of the two phases was delayed. By comparing the curves it has found that by enhancing the toluene volumetric ratio to water, the separation time has been raised. Since by increasing the volume of toluene (the disperse phase), the numbers of generated drops increase then coalescence time of drops and consequently separation time will be increase. It has been shown that in each curve after a specific impeller speed, the number of drops was increased dramatically so that there was no drops breakup, as a result the separation time was independent of the impeller speed. Therefore, in all the experiments, the separation time curves were reached a plateau. It should be noted that drops breakup was related to interfacial tension, type of fluid, and condition of flow.

The simultaneously effect of impeller speed and concentration of surfactant on phase inversion by propeller and paddle blades are illustrated in Figs. 4 and 5, respectively. These charts are related to the two sets experiments by propeller and paddle blades at seven various concentrations of surface active agent and each test was performed at 21 various impeller

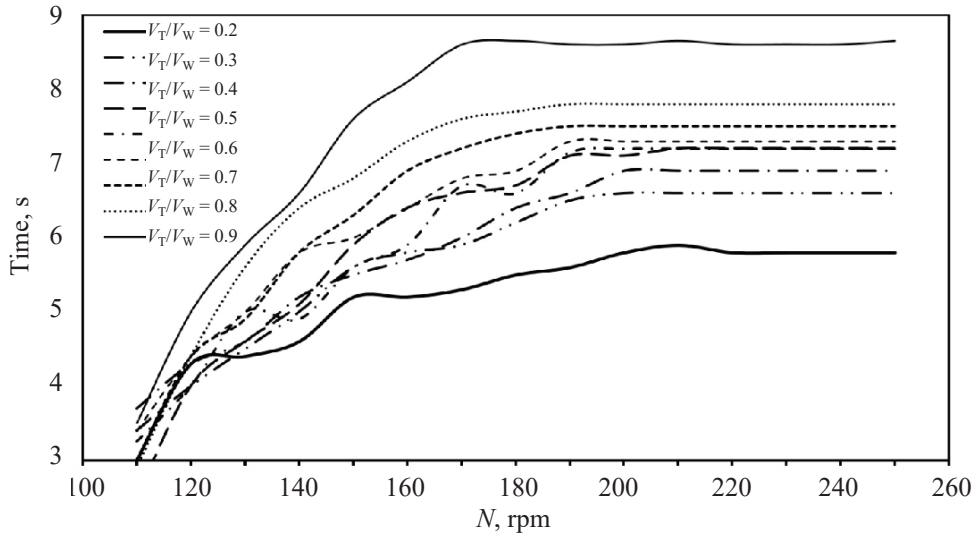

Fig. 3. The effect of impeller speed on separation time for VT/VW equal to 0.2, 0.3, 0.4, 0.5, 0.5, 0.6, 0.7, 0.8, 0.9, and 1.

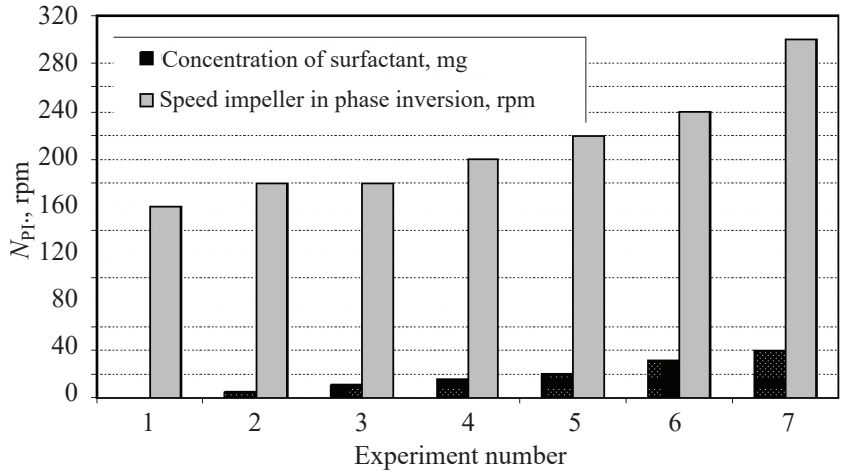

Fig. 4. The effect of impeller speed and concentration of surfactant on phase inversion by propeller blade.

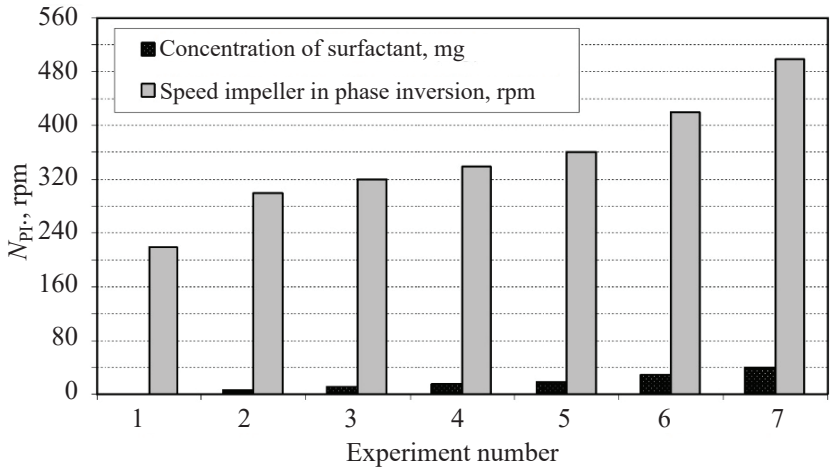

Fig. 5. The effect of impeller speed and concentration of surfactant on phase inversion by paddle blade.

speeds. Therefore, each chart was developed from 7 × 21 various experiments by various concentration of surfactant and impeller speed. Since the two-region model is based on the assumption that rates of breakup and coalescence are relatively high in the impeller and circulation regions, in which the turbulence intensity is high and low, respectively, therefore, the breakup frequency in the impeller region is much higher than in the circulation region due to existence of surfactant (SDS). Thus, the phase inversion occurred in higher impeller speeds [25]. For concentration of surface active agent higher than 40 mg, the investigation about phase inversion phenomenon was not possible, since the big amount of foam was produced. However, the mentioned range depends on operational and hydro dynamical conditions dramatically. By comparing the two bar charts, it can be seen that by increasing the surface active agent concentration, the impeller speed, at which the phase inversion phenomenon occurs, increased for both propeller and paddle blades. In the same surface active agent concentration, the phase inversion phenomenon by paddle blade occurred at higher impeller speed than that by propeller blade. On the other hand by increasing the surfactant concentration the occurrence possibility of phase inversion in propeller blade was higher than that in paddle blade. In all states, by increasing the impeller speed, the occurrence of phase inversion was increased. It must be noted that in impeller speeds lower than 100 rpm, two phases did not mix together.

In the Figs. 4 and 5 the effect of impeller speed, hold up of dispersed phase, and surface active agent concentration for two mentioned chemical systems and two types of blades are illustrated. These figures shown the impeller speed variations in round per minute

Table 5. The EViews outputs for paddle blade without SDS model

Parameter	Paddle blade without SDS	Propeller blade without SDS	Paddle blade with SDS	Propeller blade with SDS
Number of Samples	16	18	19	20
k	6.654	5.043	6.130	139.327
a	–0.649	–0.210	–0.560	–0.139
b	–0.643	–0.042	–0.409	–43.508
c	0	0	28.566	–37.937
R–squared	0.982	0.877	0.899	0.937
Adjusted *R*–squared	0.971	0.828	0.879	0.925
S.E. of regression	0.054	0.053	0.104	0.046
Sum squared residual	0.008	0.014	0.162	0.034
Log likelihood	11.077	13.936	18.281	35.323
Durbin–Watson statistic	3.291	1.590	1.772	1.309
Mean dependent variable	5.669	5.185	5.903	5.411
S.D. dependent variable	0.317	0.129	0.300	0.169
Akaike info criterion	–2.692	–2.734	–1.503	–3.132
Schwarz criterion	–2.796	–2.704	–1.304	–2.933
F–Statistic	84.767	17.942	44.980	79.933
Prob(*F*–Statistic)	0.002	0.005	0.000	0.000

at various concentration of SDS, vs. the variations of organic phase hold up. In the hold up less than 0.33 by increasing the dispersed phase hold up, the impeller speed which phase inversion occurs, decreases.

Model. As it mentioned before, the model was developed for toluene–water and butanol–water systems by paddle and propeller blades, with and without SDS. All the results for various systems are summarized in Table 5. It should be noted that all the parameters were calculated using the least squares method.

Table 5 provides the results and analysis for the developed models using the least squares method. The table includes the constant coefficients (*a*, *b*, *c*, and *k*) for each system and blade type, as well as the corresponding equations representing the relationship between the variables.

For the system with a paddle blade and without SDS, the model equation is given by Eq. (3):

$$N_{\mathrm{PI}} = 6.654\left(\Phi\right)^{-0.649}\left(\sigma\right)^{-0.643}. \quad (3)$$

The *R*-squared value (R^2) for this model is 0.97, indicating a good fit of the data. The Durbin–Watson test, which assesses autocorrelation in the residuals, yields a value of 3.291650, suggesting a good condition of the model in terms of autocorrelation. The AARD% (average absolute relative deviation) for this model is 1.14, indicating moderate agreement between the experimental and model data.

Similarly, for the system with a propeller blade and without SDS, the model equation is given by Eq. (4):

$$N_{\mathrm{PI}} = 5.043\left(\Phi\right)^{-0.210}\left(\sigma\right)^{-0.042}. \quad (4)$$

The prob (*F*-Statistic) value in Table 5 is compared to a significance level of 0.005 to assess the probability of eliminating variables. In this case, since the prob (*F*-Statistic) is 0.00523, which is greater than 0.005, there is a probability of eliminating variables. The prob (*t*-Statistic) values for coefficients *k* and *a* are less than 0.05, indicating their significance, while the prob (*t*-Statistic) for coefficient *b* is greater than 0.05, suggesting it can be eliminated from the model. Consequently, the simplified model equation becomes [Eq. (5)]:

$$N_{\mathrm{PI}} = 5.043\left(\Phi\right)^{-0.210}. \quad (5)$$

This simplified model has a prob (*F*-Statistic) of 0.000662, an indication of improved parameters

compared to the previous model. The Durbin–Watson test values for these models are 1.590870 and 1.459119, respectively, suggesting good conditions regarding autocorrelation in the residuals. The AARD% values for these models are 0.66 and 0.68, respectively, indicating good agreement between the experimental and model data.

For the system with a paddle blade and SDS, the model equation is given by Eq. (6):

$$N_{PI} = 6.130715\ (\Phi)^{-0.560623}(\sigma)^{-0.409104}(C_{SDS})^{28.56684}. \quad (6)$$

The prob (*F*-Statistic) value for this model is 0.000, indicating that there is no probability of eliminating variables. The prob (*t*-Statistic) values for all coefficients except *c* are less than 0.05, suggesting their significance. Additionally, prob (*F*-Statistic) indicates that coefficient *c* cannot be eliminated from the model. The R^2 for this model is 0.899961, indicating a good coincidence between the experimental and model results. The R^2_{adj} value, which considers the number of variables, is 0.879953, indicating the accuracy of R^2. The Durbin–Watson test yields a value of 1.772945, suggesting a good condition of the model in terms of autocorrelation. The AARD% for this model is 1.16, demonstrating good agreement between the experimental and model data.

Finally, for the system with a propeller blade and SDS, the model equation is given by Eq. (7):

$$N_{PI} = 139.3279\,(\Phi)^{-0.139056}(\sigma)^{-43.50860}(C_{SDS})^{-37.93713}. \quad (7)$$

The prob (*F*-Statistic) value for this model is 0.00, indicating that there is no probability of eliminating variables. The prob (*t*-Statistic) values for all coefficients are less than 0.05, indicating their significance. The R^2 for this model is 0.937452, indicating a good coincidence between the experimental and model results. The R^2 value is 0.925724, demonstrating the accuracy of R^2. The Durbin–Watson test yields a value of 1.309213, suggesting a good condition of the model in terms of autocorrelation. The AARD% for this model is 0.59, demonstrating good agreement between the experimental and model data.

Overall, Table 5 provides the developed models, their coefficients, statistical tests, and evaluation metrics, indicating the goodness of fit and the significance of the model parameters for each system and blade type.

CONCLUSIONS

The experiments conducted in this study aimed to investigate the phase inversion phenomenon in butanol–water and toluene–water systems, both with and without SDS as a surface-active agent. Two types of blades, paddle and propeller, were utilized in the experimental setup. The results of the study, along with the developed models for these chemical systems, revealed important insights.

It was observed that increasing the concentration of the surface-active agent led to a higher impeller speed at which the phase inversion phenomenon occurred. Simultaneously, the possibility of phase inversion decreased for both types of blades, although the increase in the paddle blade's effectiveness was more pronounced than that of the propeller blade. Recent experiments have confirmed that certain surface-active agents, including SDS, alter the hydrodynamic state, reduce turbulence transport, and decrease the rate of coalescence at the interface. Consequently, the addition of a surface-active agent reduces the coalescence rate of the dispersed phase, resulting in phase inversion occurring at higher impeller speeds.

Furthermore, the presence of a surfactant reduces turbulence transport, which, according to the two-region model, increases the fractional breakup frequency in the impeller region, surpassing the coalescence rate. The impeller speed directly influences phase inversion, with higher speeds increasing the likelihood of inversion occurrence. In the absence of a surface-active agent, the effect of impeller speed on phase inversion intensifies, making dispersion control more challenging. In a constant volumetric ratio of the dispersed phase, both the surface-active agent and impeller speed play significant roles in phase inversion and exhibit an inverse relationship with each other.

The experimental study also explored phase inversion, the separation time of phases, and the impact of the surface-active agent on phase inversion in an agitated vessel. It was observed that, beyond a certain volumetric ratio, the impeller speed directly affected phase inversion, with higher speeds increasing the probability of inversion occurrence. The effect of impeller speed on inversion became stronger, and dispersion control became more challenging with increasing volume ratios. Consequently, precise control

of impeller speed can effectively mitigate or eliminate dispersion-related issues and improve mass transfer.

Furthermore, for a specific volumetric ratio, increasing the impeller speed prolonged the phase separation time. Increasing the volumetric ratio of toluene to water and the impeller speed further delayed the separation time. However, beyond a certain impeller speed, no significant relationship was observed between separation time and impeller speed. Increasing the concentration of the surface-active agent raised the impeller speed required for phase inversion to occur. Conversely, higher surface-active agent concentrations reduced the possibility of phase inversion for both paddle and propeller blades. In a constant volumetric ratio of dispersed to continuous phase, both the surface-active agent and impeller speed had important and inversely related effects on phase inversion.

NOMENCLATURE

Φ	Dispersion phase holdup
C_{SDS}	Concentration of sodium dodecyl sulfate
AARD%	Average absolute relative deviation
a, b, c, k	Adjustable constants of impeller speed model
D	Dispersed phase
C	Continuous phase
μ	Viscosity, Pa s
ρ	Density, kg m^{-2}
σ	Interfacial tension, N/m
m_{SDS}	Mass of Sodium Dodecil Sulphate, g
N_{PI}	Impeller speed, rpm
N(k)	Number density of drops per unit volume size d_k, m^{-3}
d_{32}	The Sauter volumetric-surface mean diameter
V_{tot}	Total volume of agitated vessel, m^3
V_T	Volume of toluene, mL
V_I	Volume of impeller region, m^3
V_W	Volume of water, mL

FUNDING

The authors did not receive support from any organization for the submitted work.

CONFLICT OF INTEREST

The authors declare that they have no conflict of interest.

REFERENCES

1. Martini, P., Adamo, A., Syna, N., Boschi, A., Uccelli, L., Weeranoppanant, N., Markham, J., and Pascali, G., *Molecules*, 2019, vol. 24, p. 334. https://doi.org/10.3390/molecules24020334
2. Hasan, B.O., *Exp. Therm. Fluid Sci*., 2018, vol. 96, pp. 48–62. https://doi.org/10.1016/j.expthermflusci.2018.02.013
3. Afshar Ghotli, R., Raman, A.A., Ibrahim, S., and Baroutian, S., *Chem. Eng. Commun*., 2013, vol. 200, pp. 595–627. https://doi.org/10.1080/00986445.2012.717313
4. Widianto, A.Y., Aubin, J., Xuereb, C. and Poux, M., 2020, *Catal. Today*, 2020, vol. 346, pp. 46–57. https://doi.org/10.1016/j.cattod.2019.02.064
5. Perdih, T.S., Zupanc, M., and Dular, M., *Ultrason. Sonochem*., 2019, vol. 51, pp. 298–304. https://doi.org/10.1016/j.ultsonch.2018.10.003
6. Hiemenz, P.C. and Rajagopalan, R., *Principles of Colloid and Surface Chemistry, Revised and Expanded,* CRC press, 2016.
7. Qiu, F., Liu, Z., Liu, R., Quan, X., Tao, C., and Wang, Y., *Exp. Therm Fluid Sci*., 2018, vol. 97, pp. 351–363. https://doi.org/10.1016/j.expthermflusci.2018.04.006
8. Yang, Y., Guo, J., Ren, B., Zhang, S., Xiong, R., Zhang, D., Cao, C., Liao, Z., Zhang, S., and Fu, S., *Exp. Therm. Fluid Sci*., 2019, vol. 100, pp. 271–291. https://doi.org/10.1016/j.expthermflusci.2018.09.013
9. de Oliveira, C.B., Souza, W.J., Santana, C.F., Santana, C.C., Dariva, C., Franceschi, E., Guarnieri, R.A., Fortuny, M., and Santos, A.F., *Energy & Fuels*, 2018, vol. 32, pp. 8880–8890. https://doi.org/10.1021/acs.energyfuels.8b01227
10. Picchi, D. and Poesio, P., *Int. J. Multiphase Flow*, 2016. vol. 84, pp. 176–187. https://doi.org/10.1016/j.ijmultiphaseflow.2016.03.002
11. Binks, B.P. and Olusanya, S.O., *Chem. Sci*., 2017, vol. 8. pp.708–723. https://doi.org/10.1039/C6SC03085H
12. Asadollahzadeh, M., Torab-Mostaedi, M., Shahhosseini, S., and Ghaemi, A., *Chem. Eng. Res. Des*., 2016, vol. 105, pp. 177–187. https://doi.org/10.1016/j.cherd.2015.11.019
13. Rodger, W.A., Trice Jr, V.G., and Rushton, J.H., *Chem. Eng. Progr*., 1956, vol. 52, p. 6.

14. Selker, A.H. and Sleicher Jr, C.A., *Can. J. Chem. Eng*., 1965, vol. 43, pp. 298–301.
https://doi.org/10.1002/cjce.5450430606

15. Kato, S., Nakayama, E., and Kawasaki, J., *Can. J. Chem. Eng*., 1991, vol. 69, pp. 222–227.
https://doi.org/10.1002/cjce.5450690126

16. Efthimiadu, I., Kocianova, E., and Moore, I.P.T., *Proceedings of the 1994 ICHEME Research Event*., 1994, vol. 2, pp. 1020–1022.

17. Miller, D.J., Henning, T., and Grünbein, W., *Colloids Surf., A,* 2001, vol. 183, pp. 681–688.
https://doi.org/10.1016/S0927-7757(01)00494-0

18. Yeo, L.Y., Matar, O.K., de Ortiz, E.S.P., and Hewitt, G.F., *Chem. Eng. Sci*., 2002, vol. 57, pp. 3505–3520.
https://doi.org/10.1016/S0009-2509(02)00260-9

19. Yeo, L.Y., Matar, O.K., de Ortiz, E.S.P., and Hewitt, G.F., *J. Colloid Interface Sci*., 2002, vol. 248, pp. 443–454.
https://doi.org/10.1006/jcis.2001.8159

20. Brauner, N. and Ullmann, A., *Int. J. Multiphase Flow*, 2002, vol. 28, pp. 1177–1204.
https://doi.org/10.1016/S0301-9322(02)00017-4

21. Sajjadi, S., Zerfa, M., and Brooks, B.W., *Colloids Surf., A*, 2003, vol. 218, pp. 241–254.
https://doi.org/10.1016/S0927-7757(02)00596-4

22. Deshpande, K.B. and Kumar, S., *Chem. Eng. Sci*., 2003, vol. 58, pp. 3829–3835.
https://doi.org/10.1016/S0009-2509(03)00235-5

23. Bouchama, F., Van Aken, G.A., Autin, A.J.E., and Koper, G.J.M., *Colloids Surf., A*, 2003, vol. 231, pp. 11–17.
https://doi.org/10.1016/j.colsurfa.2003.08.011

24. Liu, L., Matar, O.K., de Ortiz, E.S.P., and Hewitt, G.F., *Chem. Eng. Sci*., 2005, vol. 60, pp. 85–94.
https://doi.org/10.1016/j.ces.2004.07.066

25. Hu, B., Angeli, P., Matar, O.K. and Hewitt, G.F., *Chem. Eng. Sci*., 2005, vol. 60, pp. 3487–3495.
https://doi.org/10.1016/j.ces.2005.02.002

26. Ioannou, K., Nydal, O.J., and Angeli, P., *Exp. Therm. Fluid Sci*., 2005, vol. 29, pp. 331–339.
https://doi.org/10.1016/j.expthermflusci.2004.05.003

27. Hu, B., Matar, O.K., Hewitt, G.F., and Angeli, P., *Chem. Eng. Sci*., 2006, vol. 615, pp. 4994–4997.
https://doi.org/10.1016/j.ces.2006.03.053

28. Piela, K., Delfos, R., Ooms, G., Westerweel, J., Oliemans, R.V.A., and Mudde, R.F., *Int. J. Multiphase Flow*, 2006, vol. 32, pp. 1087–1099.
https://doi.org/10.1016/j.ijmultiphaseflow.2006.05.001

29. Amouei, M., Khadiv, P.P., Mousavian, M., Hedayat, N., and Davoudi, A., *Iran. J. Chem. Eng.,* 2008, vol. 5, pp. 55–63.

30. Hedayat, N., Khadiv, P.P., and Mousavian, M., *Iran. J. Chem. Eng*., 2009, vol. 28, pp. 91–95.

31. Piela, K., Djojorahardjo, E., Koper, G.J.M., and Ooms, G., *Chem. Eng. Res. Des*., 2009, vol. 87, pp. 1466–1470.
https://doi.org/10.1016/j.cherd.2009.04.009

32. De, B., Mandal, T.K., and Das, G., *Chem. Eng. Res. Des*., 2010, vol. 88, pp. 819–826.
https://doi.org/10.1016/j.cherd.2010.01.003

33. Hapanowicz, J., 2010, *Flow Meas. Instrum*., vol. 21, pp. 284–291.
https://doi.org/10.1016/j.flowmeasinst.2010.03.001

34. Xu, J.Y., Li, D.H., Guo, J., and Wu, Y.X., *Int. J. Multiphase Flow*, 2010, vol. 36, pp. 930–939.
https://doi.org/10.1016/j.ijmultiphaseflow.2010.08.007

35. Preziosi, V., Perazzo, A., Caserta, S., Tomaiuolo, G., and Guido, S., *Chem. Eng*., 2013, vol. 32, pp. 1585–1590.
https://doi.org/10.3303/CET1332265

36. Asadabadi, M.R., Abolghasemi, H., Maragheh, M.G., and Nasab, P.D., *Korean J. Chem. Eng.*, 2013, vol. 30, pp. 733–738.
https://doi.org/10.1007/s11814-012-0195-9

37. Wang, W., Cheng, W., Duan, J., Gong, J., Hu, B., and Angeli, P., *Chem. Eng. Sci.*, 2014, vol. 105, pp. 22–31.
https://doi.org/10.1016/j.ces.2013.10.012

38. Perazzo, A., Preziosi, V., and Guido, S., *Adv. Colloid Interface Sci*., 2015, vol. 222, pp. 581–599.
https://doi.org/10.1016/j.cis.2015.01.001

39. Hołda, A.K. and Vankelecom, I.F., *J. Appl. Polym. Sci.,* 2015, vol. 132, p. 42130.
https://doi.org/10.1002/app.42130

40. Soin, N., Boyer, D., Prashanthi, K., Sharma, S., Narasimulu, A.A., Luo, J., Shah, T.H., Siores, E., and Thundat, T., *Chem. Commun*., 2015, vol. 51, pp. 8257–8260.
https://doi.org/10.1039/C5CC01688F

41. Li, L., Chen, M., Dong, Y., Dong, X., Cerneaux, S., Hampshire, S., Cao, J., Zhu, L., Zhu, Z., and Liu, J., *J. Eur. Ceram. Soc*., 2016, vol. 36, pp. 2057–2066.

https://doi.org/10.1016/j.jeurceramsoc.2016.02.020

42. Munirasu, S., Banat, F., Durrani, A.A., and Haija, M.A., *Desalination*, 2017, vol. 417, pp. 77–86. https://doi.org/10.1016/j.desal.2017.05.019
43. Chuesiang, P., Siripatrawan, U., Sanguandeekul, R., McLandsborough, L., and McClements, D.J., *J. Colloid Interface Sci*., 2018, vol. 514, pp. 208–216. https://doi.org/10.1016/j.jcis.2017.11.084
44. de Oliveira Honse, S., Kashefi, K., Charin, R.M., Tavares, F.W., Pinto, J.C., and Nele, M., *Colloids Surf. A*, 2018, vol. 538, p. 565, vol. 573.

    https://doi.org/10.1016/j.colsurfa.2017.11.028
45. Pierlot, C., Ontiveros, J.F., Royer, M., Catte, M., and Salager, J.L., 2018, *Colloids Surf. A*, vol. 536, p. 113, vol.124. https://doi.org/10.1016/j.colsurfa.2017.07.030
46. Binks, B.P. and Shi, H., 2019, *Langmuir*, vol. 35, pp. 4046–4057. https://doi.org/10.1021/acs.langmuir.8b04151
47. Yang, Z., Zhao, D., Xu, M., and Xu, Y., *Macromol. Rapid Commun*., 2000, vol. 21, p. 574. https://doi.org/10.1002/1521-3927(20000601)21:9<574::AID-MARC574>3.0.CO;2-O
48. Agung, I.G.N., 2011, *Series Data Analysis Using EViews,* John Wiley & Sons.
49. *Eviews 6 User's Guide,* Quantitative Micro Sftware, LLC, 2007.
50. *Eviews 4 User's Guide,* Quantitative Micro Software, 2000.